Korean Journal of Remote Sensing, Vol.24, No.5, 2008, pp.445~452

Study on Ship Detection Using SAR Dual-polarization Data: ENVISAT ASAR AP Mode

Chan-Su Yang*† and Kazuo Ouchi**

*Ocean Satellite Research Group, Korea Ocean Research & Development Institute,
1270 Sa-2-dong Sangrok-gu Ansan-city, 426-744, Korea
**Department of Computer Science, National Defense Academy,
1-10-20 Hashirimizu, Yokosuka, Kanagawa, 239-8686 Japan

Abstract : Preliminary results are reported on ship detection using coherence images computed from cross-correlating images of multi-look-processed dual-polarization data (HH and HV) of ENVISAT ASAR. The traditional techniques of ship detection by radars such as CFAR (Constant False Alarm Rate) rely on the amplitude data, and therefore the detection tends to become difficult when the amplitudes of ships images are at similar level as the mean amplitude of surrounding sea clutter. The proposed method utilizes the property that the multi-look images of ships are correlated with each other. Because the inter-look images of sea surface are covered by uncorrelated speckle, cross-correlation of multi-look images yields the different degrees of coherence between the images and water. In this paper, the polarimetric information of ships, land and intertidal zone are first compared based on the cross-correlation between HH and HV images. In the next step, we examine the technique when the dual-polarization data are split into two multi-look images. It was shown that the inter-look cross-correlation method could be applicable in the performance improvement of small ship detection and the land masking. It was also found that a simple combination of coherence images from each co-polarised (HH) inter-look and cross-polarised (HV) inter-look data can provide much higher target-detection possibilities.

Key Words : Ship detection, Cross-correlation, multi-look processing, ship detection, speckle noise, synthetic aperture radar (SAR), ENVISAT-ASAR, dual-polarisation.

1. Introduction

Dual polarisation data are important for a wide range of applications such as estimation of soil moisture, forest and vegetation studies, sea ice applications, etc. Multi-polarization and polarimetric data are expected to allow the user to exploit various polarization combinations to optimize ship detection applications. The Advanced Synthetic Aperture Radar (ASAR) is one of the instruments aboard the Environmental Satellite ENVISAT and provides dual-channel SAR data. In an additional ASAR measurement mode, called Alternating Polarisation Mode (AP Mode), which employs a modified

Received September 26, 2008; Revised October 7, 2008; Accepted October 17, 2008.
† Corresponding Author: Chan-Su Yang (yangcs@kordi.re.kr)

ScanSAR technique, it scans between two polarisations, HH (H transmit and H receive) and VV (V transmit and V receive), within a pre-selected single swath. In addition, there are two cross-polar modes, where the transmit pulses are all H or all V polarisation, with the receive chain operating alternatively in H and V, as in the co-polar mode.

Several papers treat different methods for detection of ships in SAR images (Gredanus and Kourti 2006; Li and Chong 2008; Liao *et al.* 2008; Liu *et al.*, 2005). However, detection ability of ocean features decreases with high sea states due to higher level of clutter. Thus, an alternative method is to identify ships from their wake lines. This method cannot, of course, be used unless the wake images are clearly visible. There is also the method based on the coherence image from two multi-look images, in which the degree of coherence between ships is high (Ouchi *et al.* 2004).

In ship detection using SAR, the detection of smaller ships, the masking of land in the areas of many islands and intertidal zone, and the discrimination of ship-like surface features such as floating aids to navigation (small, medium and large buoys) is remained to be resolved.

This paper presents two case studies of ship detection approach. We first consider the polarisation property for ships and land area including intertidal zone using cross-correlation method. Masking of land is performed using the method without any reference data. In the second part, we develop the previous method of ship detection by cross-correlating multi-look co-polarisation images (Ouchi *et al.* 2004) to a step further, and examine a technique by cross-correlation of the multi-look dual-polarisation images.

2. Alternating Polarisation (AP) Mode of ENVISAT Advanced Synthetic Aperture Radar (ASAR)

The Advanced Synthetic Aperture Radar (ASAR), operating at C-band (5.331 GHz), one of the 10 instruments on board of ENVISAT, is equipped with an active phased array antenna of 320 transmit/ receive modules, organised in 32 rows to produce a versatile position of the image swath by beam steering in elevation (Rosich *et al.* 2003).

In addition, the instrument is designed to provide a large degree of operational flexibility, acquiring science data in 5 different modes. The Image Mode (IM) generates high spatial resolution data, in HH (H transmit and H receive) or VV polarization, over one of seven available swaths located over a range of incidence angles spanning 15° to 45°. The Wave Mode (WM) generates vignettes of 10 km by 10 km spaced 100 km along-track, in HH or VV polarisation. The position of the vignette can be selected to alternate between the centre of any two of the seven swaths. The Wide Swath Mode (WSM) and Global Monitoring Mode (GMM) are based on the ScanSAR technique using five sub-swaths (across-track coverage of 400 Km) either in HH or in VV polarisation. The first one is a high resolution mode, for which typical products of 150 m geometric resolution are generated, while the second one is a low rate mode, which allows for a whole orbit operation at the cost of reducing the resolution to ~1Km. The Alternating Polarisation (AP) Mode provides two simultaneous images from the same area in HH and VV polarizations, HH and HV or VV and VH, using the ScanSAR technique, with the same imaging geometry as Image Mode and similarly high spatial resolution (Fig. 1) (Rosich *et al.* 2003; Small *et al.* 2004). Alternating Polarization mode is 56 - 100 km across track depending on sub-swath.

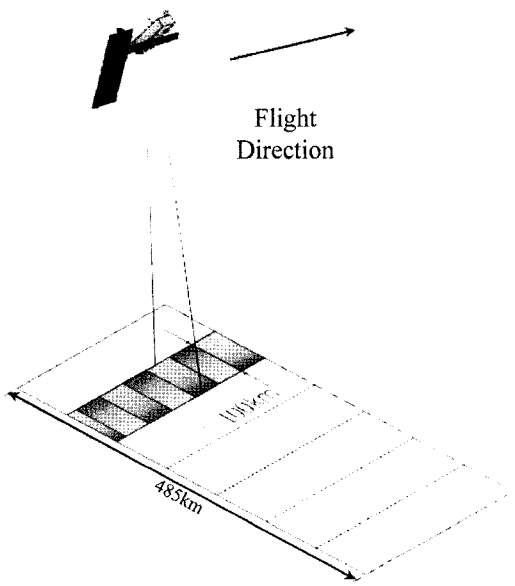

Fig. 1. ENVISAT ASAR alternating polarization mode.

Along track coverage depends on the requested time interval.

3. Data (ASA_APH_0P) and study area

ASAR Level 0 data of alternating polarization mode used here are AP Crosspolar H Level 0 (HH/HV= H transmit H and V received), obtained on December 4, 2006. The level 0 data were processed to the ground range intensity (GRD) image by the SAR processor as shown in the right of Fig. 2.

Fig. 2 shows a sketch map of the research area as well as an approximate outline of an IS6 descending swath with the incidence angle range from 39.1° to 42.8°. The image size is approximately 152 km and 73 km in azimuth and range directions, respectively. Both the azimuth and range pixel spacing are 12.5 m. In the figure, the circle area represents an observation site of wind and wave, and at the time half hour before and after the data acquisition (01:32 GMT), the wind speeds were 6.2 m/s and 7.0 m/s, and the significant wave heights were 0.4 m and 0.3 m, respectively.

In this study, a small area (rectangle box) of the ASAR APH intensity image was selected to examine the performance of a ship detection approach from a dual polarisation data using the multi-look cross-correlation method. The area of 290 × 290 pixels includes 3 different ships (warship, tug boat and container shown in Fig. 3), island and intertidal zone.

Validation data include the names of the ships, call

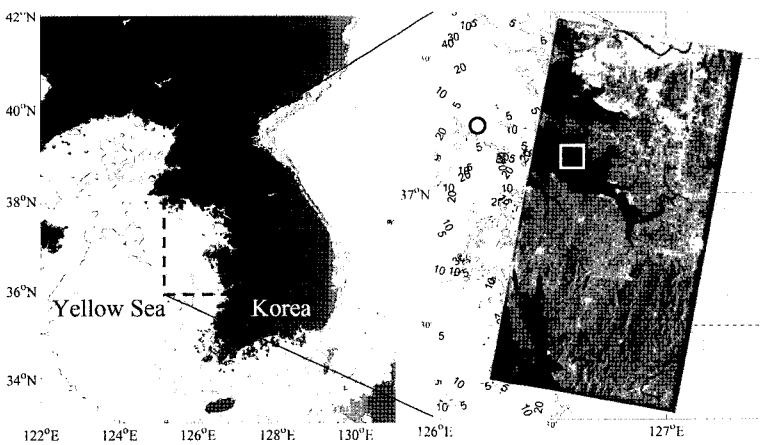

Fig. 2. Area of interest for ENVISAT ASAR AP data analysis. The IS6 APH swath coverage is shown by the rectangle in the left and the right is the intensity image acquired on December 4, 2006. The circle and the small rectangle in the right represent a site of meteorological observation and a test area of ship detection, respectively.

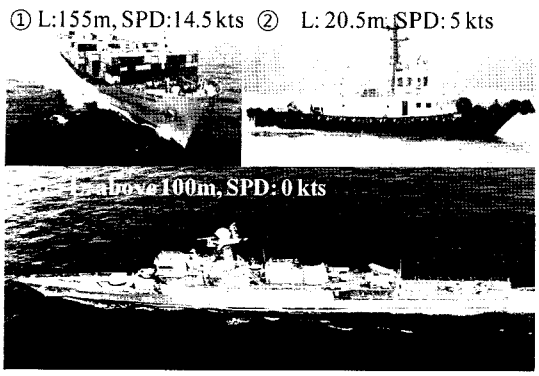

Fig. 3. Ships used as the ground truth in this study. As for the positions of the circled numbers, refer to Fig. 5.

sign, latitude/longitude position, and ship size and type, that are tracked by Automatic Identification System (AIS) and Vessel Traffic Service (VTS).

4. Method

In order to compute the inter-look and inter-polarization cross-correlation functions, the total 8 images of the same area were processed. When multi-look processing is used, there is a positional difference in the inter-look images of moving ships due to the center time difference between the sub-reference signals. In the multi-look processing used in this study, the bandwidth of the sub-reference signal was 682 Hz, and the Doppler center frequencies were -477.5 Hz and 204.5 Hz (2-look processing). The relation between the Doppler frequencies f_D and azimuth time t is given by

$$\Delta t = \frac{\lambda R}{2V^2} f_D \qquad (1)$$

where λ is the radar wavelength, R is the slant-range distance, and V is the platform velocity. For this particular data set, the relative platform velocity is 7.1 km/s and slant-range distance is 1,044 km with the incidence angle of 40.1° at the center of the image of Fig. 1 (swath area). From Eq. (1), then, the azimuth integration time of each sub-reference signal or the inter-look center time difference become 0.4 s. The fastest speed of a ship was the tanker in Fig. 3 with 14.5 knots (7.3 m/s), so that the inter-look image position differs by 2.9 m. Thus, there is a difference in the ships' image positions between looks, but the difference is not large enough to affect the inter-look cross correlation function.

The correlation between two signals is a standard approach to feature extraction. The inter-look cross-correlation function is defined as

$$C = \frac{\langle I_1 I_2 \rangle}{\langle I_1 \rangle \langle I_2 \rangle} \qquad (2)$$

where I_j (j =1,2) is the look j image intensity within a moving window, and the angular brackets indicate averaging.

The cross-correlation can be computed in either the spatial domain directly or in the Fourier domain. The frequency domain was used here, but normalized cross correlation was computed in the spatial domain, because the transform domain does not have a correspondingly simple and efficient expression on it.

The scene generation from multi-look processing is illustrated in Fig. 4. The two multi-look images are generated in both single-look complex (SLC) and multi-look ground range intensity (GRD) products for each polarization mode.

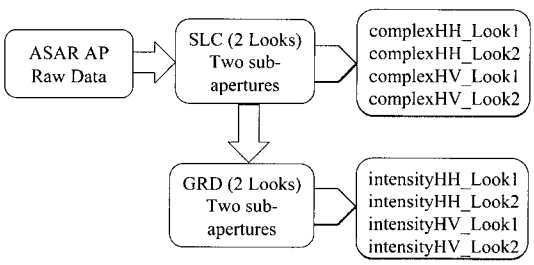

Fig. 4. Procedure of ENVISAT ASAR AP data processing.

5. Ship detection using dual polarization data: HH & HV

Fig. 5 shows HH and HV sub-images of ENVISAT ASAR APH. The top-right of the figure is the area of island and intertidal zone. Three ships marked as 1, 2 and 3 are visible as bright areas in the HH image, while only two large ships marked 1 and 2 are visible in the HV image.

In general, C band imagery in HH polarization is preferred for ship detection because the background clutter is smaller than that at VV polarization, and hence the ship-sea contrast is usually higher. The cross-polarised return is usually weaker than co-polarization returns, and often associated with multiple scattering due to multiple and volume scattering.

The top of Fig. 6 is the coherence image computed from the two images of Fig. 5 with a 3 × 3 pixel moving window. Because two ships labelled 1 and 3 have high intensity values in both the HH and HV images, they can easily be extracted from the coherence image. The ship image labelled 2 has lower intensity and contaminated with noise. The complex image of the smaller ship, i.e. the ship No.2 did not show high coherence to be distinguished from sea images. The bottom-left and bottom-right are the coherence images after thresholding the top coherence image with the sensitivity thresholds of 1.4 and 1.0, where the thresholding values are determined by the Sobel method (Sobel 1995). This method ignores all edges that are not stronger than a threshold, which results from the multiplication of the sensitivity threshold and the threshold of the Sobel method.

From the figure, it is obvious that the noise is reduced, and the island and intertidal zone are masked out. However, the breakwater built on the island is also extracted during the normal processing as shown in the bottom-right of Fig. 6. If the edge factor is reduced to 0.6, the four probable ship targets including the ship No. 2 could be detected but the noise will be increased. Thus, it is not easy to extract ships from the all unidentified targets including floating aids to navigation, although the intertidal and island areas could be removed.

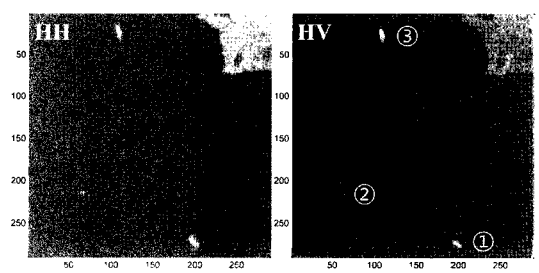

Fig. 5. Sub-images of ENVISAT ASAR APH (HH/HV) as in the same area of the rectangle of Fig. 2. Note that all three ships are visible in HH image.

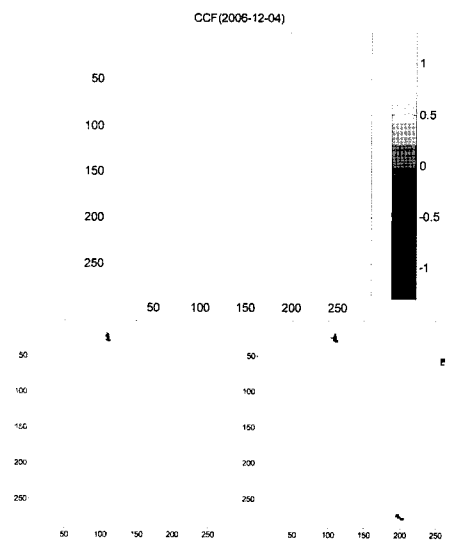

Fig. 6. Coherence image (top) computed by a moving window of size 3 × 3 pixels for the images of Fig. 5. The images in the bottom row are those after thresholding with the sensitivity thresholds for the Sobel method, with the sensitivity thresold level 1.4 (left) and 1 (right).

6. Ship detection using multi-look SAR images of dual polarization data: HH & HV

Fig. 7 shows multi-look HH and HV sub-images of ENVISAT ASAR APH. The left column is the look 1 intensity images and the right is those of the look 2.

The left and right of Fig. 8 are the coherence images computed from each multi-look HH and HV images of Fig. 7 with a 3 × 3 pixel moving window. Data acquired in the look 1 and look 2 images of ships at HH polarization are highly correlated, whereas those at HV polarization are very poorly correlated.

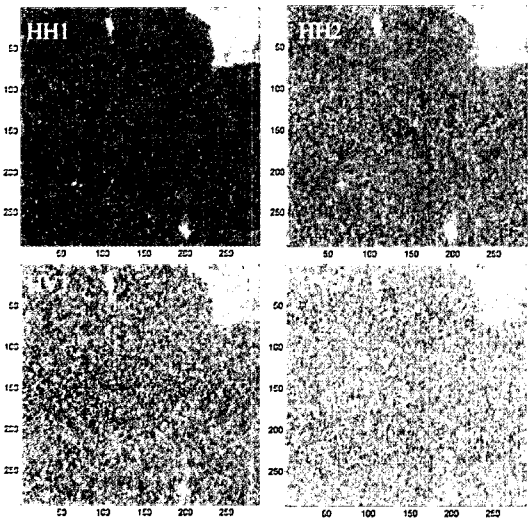

Fig. 7. Multi-look HH (top row) and HV (bottom row) images of ENVISAT ASAR APH.

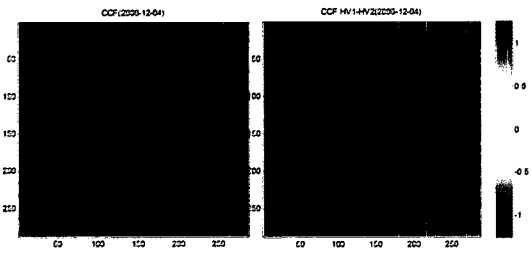

Fig. 8. Coherence images computed with a moving window of size 3 × 3 pixels from the top-row (HH1/HH2) and bottom-row (HV1/HV2) images of Fig. 7, respectively.

Fig. 9 is the coherence images computed from the look 1 images of HH and HV of Fig. 7 with a 3 × 3 pixel moving window.

Performance result for the algorithm efficiency comparison is presented in Table 1. High performance by coherence image (HH1/HH2) is apparent in ship detection while land masking is effective in the coherence image (HH1/HH2).

In Fig. 9, the correlation between the two different

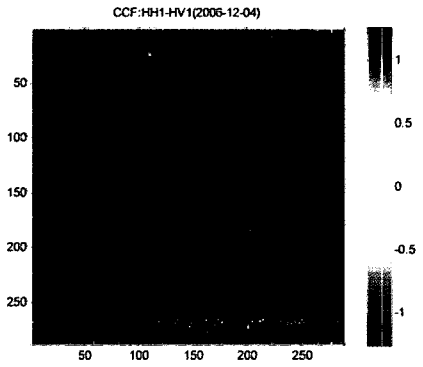

Fig. 9. Coherence image computed with a moving window of size 3 × 3 pixels from the left-column images (HH1/HV1) of Fig.7.

Table 1. Performance comparisons for ship detection and masking in SNR (Signal to background Noise Ratio)

	HH& HV	HH1& HH2	HV1& HV2	HH1& HV1	HH2& HV2
Ship 1	185.78	209.13	7.58	279.17	419.25
Ship 2	4.66	4.34	4.96	6.44	6.00
Ship 3	111.07	185.78	119.07	335.20	335.20
Masking	8.29	6.57	5.86	4.92	5.20

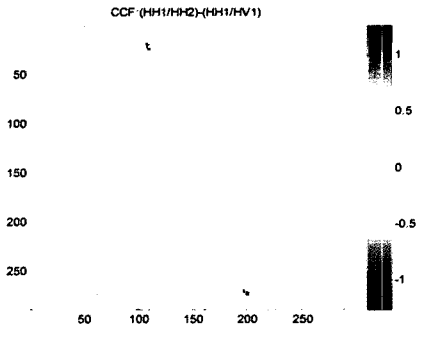

Fig. 10. Coherence image (HH1/HH2) - coherence image (HH1/HV1).

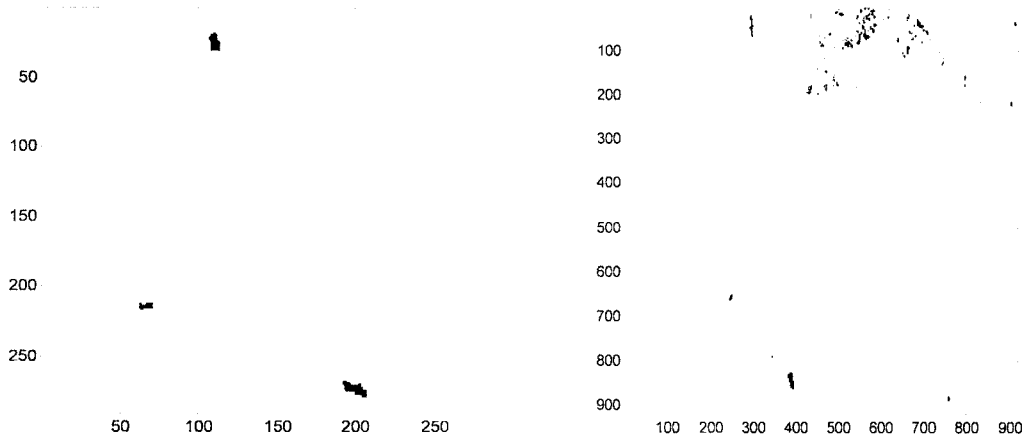

Fig. 11. Thresholded image (left) of the coherence difference image of Fig. 10 and result image (right) obtained from the same method and area for SLC data.

polarization channels has both positive and negative signatures. It is then possible to enhance the cross-correlation values using the maximum coherence image (HH1/HH2) and the minimum coherence image (HH1/HV1). The difference between two coherence images, (HH1/HH2) - (HH1/HV1), reveals the high contrasts of ships against the ocean clutter background as shown in Fig. 10. The method, calculated for complex images as in the previous studies (Iehara *et al.* 2001; Ouchi *et al.* 2004), could help the visual interpretation, but does not result in performance improvement of ship detection.

Fig. 11 is the thresholded images for the difference image between two coherence images, HH1/HH2 and HH1/HV1 for each GRD and SLC images. All three ships are well recognized in the left image, but the right includes many noise.

7. Results and Discussions

In this study, ship detection by the inter-look cross-correlation method was examined using the ENVISAT ASAR data. Since the west coast waters of Korea are occupied by many islands and intertidal zones, and used widely as navigational channels, the inter-look coherence technique could be useful in extracting ships from all ship-like candidates. The proposed method was applied to the HH and HV polarization combinations, and yielded reasonable results in the performance improvement of small ship detection and the land masking.

Further quantitative evaluation is being planned based on the comparison of other AP data with the simultaneous sea truth of several ships of different sizes and floating aids.

Acknowledgement

This work was supported by the Basic Research Project, "Development of Management and Restoration Technologies for Estuaries" of KORDI and the Public Benefit Project of Remote Sensing, "Satellite Remote Sensing for Marine Environment" of Korea Aerospace Research Institute. ENVISAT ASAR data were provided by the European Space Agency under the ESA Cat-1 Scheme ID 3853.

References

Gredanus, H., and N. Kourti, 2006. Finding of the DECLIMS project - detection and classification of marine traffic control, *Proceedings of SEASAR 2006*, 23-26 January 2006, Frascati, Italy (ESA SP-613).

Iehara, M., K. Ouchi, I. Takami, K. Morimura, and S. Kumano, 2001. Detection of ships using cross-correlation of split-look SAR images, *International Geoscience and Remote Sensing Symposium*, 9-13 July 2001, Sydney, Australia.

Li, X., and J. Chong, 2008. Processing of Envisat alternating polarization data for vessel detection, *IEEE Geoscience Remote Sensing Letters*, 5(2): 271-275.

Liao, M., C. Wang, and L. Jiang, 2008. Using SAR images to detect ships from sea clutter, *IEEE Geoscience Remote Senssing Letters*, 5(2): 194-198.

Liu, C., P. W. Vachon, and G. W. Geling, 2005. Improved ship detection with airborne polarimetric SAR Data, *Canadian Journal of Remote Senssing*, 31(1): 122-131.

Ouchi, K., S. Tamaki, H. Yaguchi, and M. Iehara, 2004. Ship detection based on coherence images derived from cross correlation of multi-look SAR images, *IEEE Transactions on Geoscience Remote Senssing*, 1(6): 184-187.

Rosich, B., M. Zink , R. Torres, J. Closa , C.Buck, 2003. ASAR instrument performance and product status, *International Geoscience and Remote Sensing Symposium*, 21-25 July 2003, Toulouse, France.

Small, D., B. Rosich E. Meier, D. Nüesch, 2004. Geometric calibration and validation of ASAR imagery, *Proceedings of CEOS SAR Workshop*, 27-28 May 2004, Ulm, Germany.

Sobel, D., 1995. *Longitude*, Walker & Company, New York, USA.